Proc. Natl. Acad. Sci. USA
Vol. 93, pp. 9420–9424, September 1996
Biochemistry

The structure of bovine F_1-ATPase complexed with the peptide antibiotic efrapeptin

(crystal structure/ATP synthesis/ATP hydrolysis)

JAN PIETER ABRAHAMS, SUSAN K. BUCHANAN*, MARK J. VAN RAAIJ, IAN M. FEARNLEY, ANDREW G. W. LESLIE, AND JOHN E. WALKER†

Medical Research Council Laboratory of Molecular Biology, Hills Road, Cambridge CB2 2QH, United Kingdom

Communicated by Henry A. Lardy, University of Wisconsin, Madison, WI, May 23, 1996 (received for review March 5, 1996)

ABSTRACT **In the previously determined structure of mitochondrial F_1-ATPase determined with crystals grown in the presence of adenylyl-imidodiphosphate (AMP-PNP) and ADP, the three catalytic β-subunits have different conformations and nucleotide occupancies. AMP-PNP and ADP are bound to subunits β_{TP} and β_{DP}, respectively, and the third β-subunit (β_E) has no bound nucleotide. The efrapeptins are a closely related family of modified linear peptides containing 15 amino acids that inhibit both ATP synthesis and hydrolysis by binding to the F_1 catalytic domain of F_1F_o-ATP synthase. In crystals of F_1-ATPase grown in the presence of both nucleotides and inhibitor, efrapeptin is bound to a unique site in the central cavity of the enzyme. Its binding is associated with small structural changes in side chains of F_1-ATPase around the binding pocket. Efrapeptin makes hydrophobic contacts with the α-helical structure in the γ-subunit, which traverses the cavity, and with subunit β_E and the two adjacent α-subunits. Two intermolecular hydrogen bonds could also form. Intramolecular hydrogen bonds probably help to stabilize efrapeptin's two domains (residues 1–6 and 9–15, respectively), which are connected by a flexible region (βAla-7 and Gly-8). Efrapeptin appears to inhibit F_1-ATPase by blocking the conversion of subunit β_E to a nucleotide binding conformation, as would be required by an enzyme mechanism involving cyclic interconversion of catalytic sites.**

The efrapeptins are a family of closely related peptide antibiotics from the soil hyphomycetes *Tolypocladia* (refs. 1 and 2; Fig. 1). They inhibit photophosphorylation in plants and bacteria (3, 4) and oxidative phosphorylation in mitochondria (5, 6) and in some (3, 7), but not all (8), bacteria. They do so by binding to a unique site in the F_1 catalytic domain of F_1F_o-ATP synthase (9). Both in intact bovine mitochondrial ATP synthase and in the soluble F_1-ATPase, efrapeptin binds with a K_d of $\approx 10^{-8}$ M (9). Inhibition by the peptide of steady-state ATP hydrolysis is not affected by compeptition with ATP, whereas inhibition of steady-state ATP synthesis in F_1F_o-ATP synthase is competitive with ADP or phosphate (9). The association rate of efrapeptin and F_1-ATPase is unaffected by high concentrations of ADP, but it decreases in the presence of phosphate. Therefore, the efrapeptin binding site may overlap with the phosphate-binding site, but not with the ADP site (10).

The ATP synthase complex has three β-subunits, each containing a catalytic site to which nucleotides bind (11). In the atomic structure of bovine mitochondrial F_1-ATPase (12), the three β-subunits alternate with the three α-subunits about a central axis of six-fold pseudosymmetry provided by an α-helical region in the single γ-subunit. The three catalytic sites are found at interfaces between β- and α-subunits. Each β-subunit has a different conformation and nucleotide occupancy. One β-subunit (β_{TP}) contains bound adenylyl-imidodiphosphate (AMP-PNP), the second (β_{DP}) has bound ADP, and, despite the presence of excesses of both nucleotides in the crystallization medium, no nucleotide is bound to the third subunit (β_E). The α-subunits are denoted α_{TP}, α_{DP}, and α_E according to the catalytic site to which they contribute. During catalysis, the conformations of the three β-subunits could be interconverted by rotation of the central α-helical structure relative to the surrounding α- and β-subunits. Therefore, the structure supports a catalytic mechanism involving cyclic interconversion of the three catalytic sites (13). If this interpretation of the structure is correct, it should also explain the mechanism of action of inhibitors of F_1-ATPase. In this paper, we describe the structure of the bovine F_1-ATPase–efrapeptin complex determined by x-ray crystallography with results that are consistent with a cyclic catalytic mechanism.

MATERIALS AND METHODS

Crystallization. Samples of efrapeptin from *Tolypocladium inflatum* were generous gifts from Lilly Research Laboratories (Indianapolis). The samples and efrapeptins bound to F_1-ATPase were analyzed by reverse-phase HPLC and electrospray ionization-mass spectrometry (14). Nucleotide-free bovine F_1-ATPase (15) was isolated in a buffer consisting of 100 mM Tris·sulfate (pH 8.0), 50% glycerol (wt/vol), and 4 mM EDTA. This solution (protein concentration 10 mg/ml; 100 vol) was mixed at room temperature with an ethanolic solution of efrapeptin (20 mg/ml; 1 vol). After 1 h, AMP-PNP was added to a final concentration of 1 mM. One hour later, the solution was mixed with an equal volume of crystallization buffer (15) containing 14% PEG 6000, but no nucleotides, and dialyzed against buffer containing AMP-PNP and ADP (both at 100 μM). Crystals grew at 23°C in 6–8 weeks.

Data Collection. Immediately before data collection, the glycerol concentration in the crystallization buffer was increased from 0 to 20% in 5% steps. One crystal was cooled rapidly to 100 K, and x-ray diffraction data were collected at the Synchrotron Radiation Source (Daresbury, U.K.). The unit cell dimensions of the crystal were 285.7 × 107.4 × 139.5 Å^3 (1 Å = 0.1 nm), and its anisotropic mosaic spread varied from 0.25 to 0.4°. Because of time constraints, only 86% of the unique data to 3.1 Å was measured, spread uniformly through reciprocal space by leaving 5° gaps between wedges of data of 10–15°. Reflections were integrated with the computer pro-

The publication costs of this article were defrayed in part by page charge payment. This article must therefore be hereby marked "*advertisement*" in accordance with 18 U.S.C. §1734 solely to indicate this fact.

Abbreviation: AMP-PNP, adenylyl-imidodiphosphate.

Data deposition: The atomic coordinates and structure factors have been deposited in the Protein Data Bank, Chemistry Department, Brookhaven National Laboratory, Upton, NY 11973 (reference 1EFR).

*Present address: Howard Hughes Medical Institute, University of Texas, South Western Medical Center, Dallas, TX 75235-9050.

†To whom reprint requests should be addressed. e-mail: walker@mrc-lmb.cam.ac.uk.

```
        1                5                10               15
C   Ac-Pip-Aib-Pip-Aib-Aib-Leu-βAla-Gly-Aib-Aib-Pip-Aib-Gly-Leu-Aib-X
D   Ac-Pip-Aib-Pip-Aib-Aib-Leu-βAla-Gly-Aib-Aib-Pip-Aib-Gly-Leu-Iva-X
E   Ac-Pip-Aib-Pip-Iva-Aib-Leu-βAla-Gly-Aib-Aib-Pip-Aib-Gly-Leu-Iva-X
F   Ac-Pip-Aib-Pip-Aib-Aib-Leu-βAla-Gly-Aib-Aib-Pip-Aib-Ala-Leu-Iva-X
G   Ac-Pip-Aib-Pip-Iva-Aib-Leu-βAla-Gly-Aib-Aib-Pip-Aib-Ala-Leu-Iva-X
```

FIG. 1. Covalent structures of efrapeptins C, D, E, F, and G. Pip, Aib, and βAla are pipecolic acid, α-aminoisobutyric acid, and β-alanine, respectively. The leucine, pipecolic acid, and alanine residues have the L-configuration. Substituent X is isobutyl[2,3,4,6,7,8-hexahydro-1-pyrrolo]1,2-α[pyrimidinyl]ethylamine, and Ac is acetyl (see refs. 1 and 2).

gram MOSFLM (16) and the data were processed with programs from the Collaborative Computing Project No. 4 suite (17).

Structure Solution and Refinement. Programs from the TNT suite (18) were used for all refinements. One percent of the data (692 reflections) was reserved for the free R-factor calculation (19) and was excluded from all refinement, including the initial rigid body refinement. A starting model of F_1-ATPase (12) that had been refined against the data for F_1-ATPase determined at 2.8 Å resolution (crystallographic R-factor 17.2%; R-free 25.4%; 603 water molecules; 0.016 Å and 2.91° rms deviations for bonds and angles, respectively) was subjected to rigid body refinement. This model was used to remove the anisotropy of the overall temperature factor of the crystallographic data with the computer program COMPAR (20). As a result, both the R-factor and the R-free decreased by 1.5%. Efrapeptin C was built into a sigma A weighted difference density map (21) with the computer graphics program O (22). Some side chains around the efrapeptin-binding site were repositioned, and some loops, mainly at hinge-points between the rigid groups used in the refinement, were rebuilt. The stereochemistry of the efrapeptin was restrained with bond lengths and angles from computer programs in the TNT suite. Because the poorly ordered parts of the crystal could not be modeled adequately with a bulk solvent correction, the low resolution cut-off was set to 5.5 Å. However, in the calculation of the maps used for rebuilding, the low resolution data were included.

To prevent model bias from the limited resolution of the data, the atomic model was subjected to alternate rounds of refinement with likelihood weighted local symmetry restraints either to the F_1-ATPase structure, or, in the case of the α- and β-subunits, to the other copies present in the asymmetric unit. This approach required modifications to the noncrystallographic symmetry module of the TNT program suite (see ref. 23). When the restrained refinement of the atomic positions of the protein, efrapeptin, and nucleotides had converged, the complete model, including water molecules, was subjected to a real space refinement of all atomic positions and temperature factors. This procedure improved the geometry of the model further, and reduced R-free by 0.2%. The crystallographic data are summarized in Table 1.

RESULTS AND DISCUSSION

Structural Analysis and Data Quality. A sigma A weighted electron density map (21) of the differences between the rigid body refined F_1-ATPase and the F_1-ATPase–efrapeptin complex showed the location of the antibiotic clearly (Fig. 2*A*). The final model has excellent stereochemistry (0.006 Å rms deviation of bond lengths, 1.75° rms deviation of bond angles). The main chain torsion angles of 86.8% of the residues are in the most favored regions of the Ramachandran plot, 12.8% of the residues are in additional allowed regions, and 0.4% of the residues are in generously allowed regions (24). The final R-factor and free R-factor (17.7% and 22.5%, respectively) allow the mode of efrapeptin binding to be interpreted with a high level of confidence.

Because of the limited resolution of the x-ray data, it was important to provide adequate restraints during refinement. The application of the likelihood weighted noncrystallographic symmetry restraints and the restraints to the F_1-ATPase structure (12) proved to be valuable. This was demonstrated by subjecting the final model to refinement without such restraints. Although neither temperature factors nor water molecules were refined, the R-factor dropped to 17.0% with very good stereochemistry, but the R-free increased to 25.4%.

Global Structural Changes in F_1-ATPase. Small but significant differences were observed in the relative orientations of the subunits and their domains in the structure of the F_1-

Table 1. Crystallographic data for the bovine F_1-ATPase–efrapeptin complex as a function of the resolution

Resolution, Å	R_{sym}*	⟨F/o⟩†	Multiplicity	Completeness	R_f‡	R_{free}§
15–5.5	0.058	70	2.6	0.97	—	—
5.5–4.6	0.072	48	2.7	0.96	0.165	0.205
4.6–4.0	0.075	43	2.7	0.90	0.165	0.190
4.0–3.6	0.087	33	2.5	0.87	0.190	0.235
3.6–3.35	0.111	24	2.5	0.85	0.220	0.295
3.35–3.1	0.152	16	2.5	0.83	0.245	0.275
Overall	0.079	37	2.6	0.86	0.177	0.225

*$R_{sym} = \Sigma\ 1\ (I-\langle I\rangle)\ 1/\Sigma\ (I)$, where I = observed density, and $\langle I\rangle$ is the mean density from multiple measurements after rejections (0.0015% of the data were rejected).

†The mean of the structure factor amplitude over the standard deviation as estimated from counting statistics.

‡The crystallographic R-factor.

§The free R-factor of 1% of the data not included in the refinement.

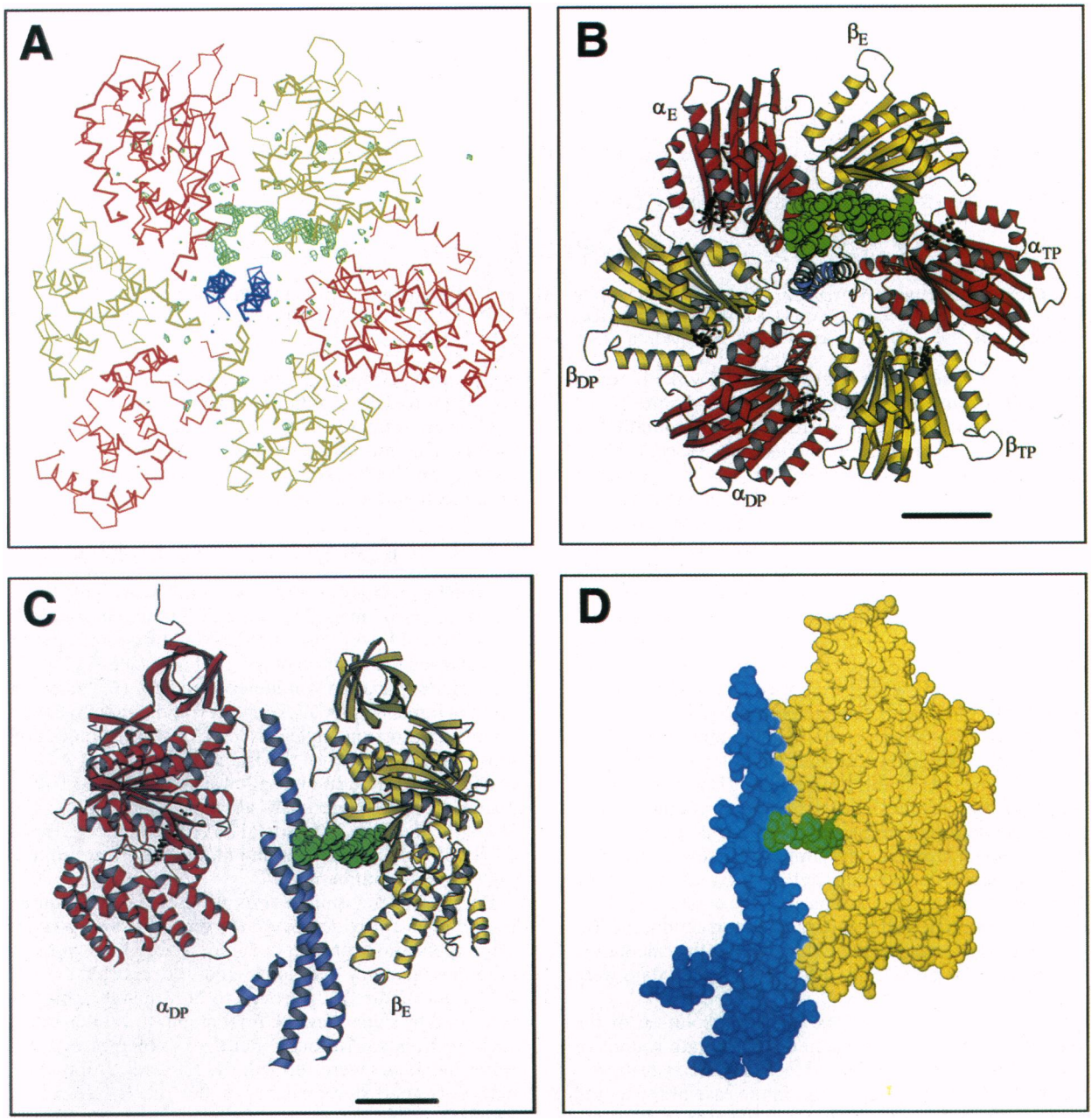

FIG. 2. The structure of the bovine F_1-ATPase–efrapeptin complex. The α-, β-, and γ-subunits are colored red, yellow, and blue, respectively, and efrapeptin is green. The scale bars represent 20 Å. (*A*) F_1-ATPase complex viewed away from the membrane to which F_1-ATPase is bound in intact ATP synthase, with the positive electron density difference corresponding to efrapeptin. The Cα backbones of the three α-subunits alternate with those of the three β-subunits around the central α-helical coiled-coil in the unique γ-subunit. The contour level of the difference map was set to 1.2 σ of the $2F_o$-F_c map. (*B* and *C*) The α-, β-, and γ-subunits in ribbon representation surround a space-filling representation of efrapeptin. (*B*) The complex viewed from the same aspect as in *A*, showing bound efrapeptin with the nucleotide-binding domains of α- and β-subunits and the central α-helical coiled-coil in the γ-subunit. (*C*) Side view of F_1-ATPase with bound efrapeptin, showing subunits α_{DP} and β_E and three α-helical segments in the γ-subunit. (*D*) Space filling model of efrapeptin interacting with the β_E and γ-subunits.

ATPase–efrapeptin complex in comparison with that of F_1-ATPase. These differences were apparent from the behavior of R-free in rigid body refinements. After correction for the anisotropy of the overall temperature factor of the data (20), the initial R-factor of the model of F_1-ATPase placed in the unit cell of the F_1-ATPase–efrapeptin complex was 38.1%. Upon refinement of the entire enzyme as a single rigid body, the R-free fell to 26.6%. Refinement of the individual subunits of F_1-ATPase as rigid bodies decreased R-free to 24.6%, and after breaking the subunits into rigid domains, R-free fell to 23.2%. After inclusion of efrapeptin and model rebuilding, refinement decreased R-free to 22.5%. The rms deviation of the Cα atoms between F_1-ATPase and the final model of the F_1-ATPase–efrapeptin complex is 0.31 Å. The observed differences could have been caused by the binding of efrapeptin to F_1-ATPase, or they could have arisen by freezing the crystal.

The Efrapeptin-Binding Site. The F_1-ATPase complex has a large central cavity traversed by an α-helical structure in the γ-subunit (12). The single efrapeptin molecule in the F_1-ATPase–efrapeptin complex binds in this cavity, where it makes contacts with the γ-, β_E-, α_E-, and α_{TP}-subunits (see Figs. 2 *B–D* and 3). Antibiotic binding is accompanied by small changes around the central cavity. To accommodate the antibiotic, the side chains of β_E-Phe326, β_E-Asp352, β_E-

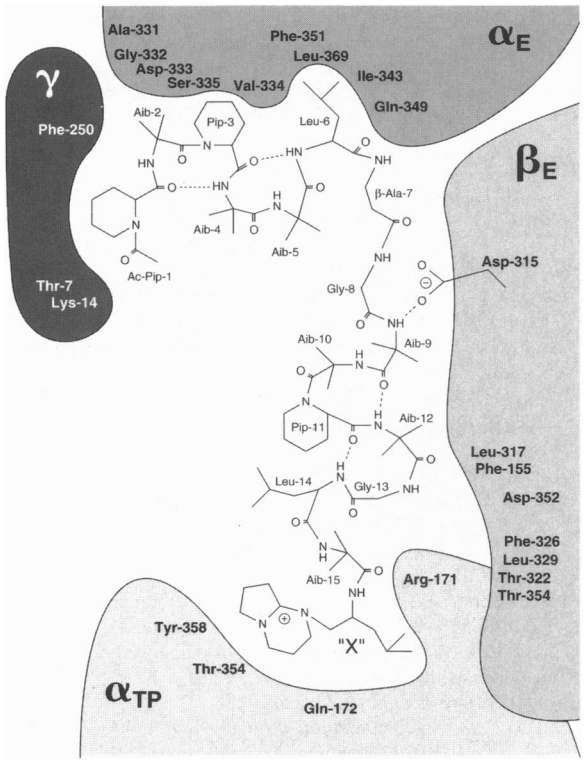

FIG. 3. Schematic summary of binding of efrapeptin to bovine F_1-ATPase. The binding site is formed by residues from subunits α_E, α_{TP}, β_E, and γ of F_1-ATPase. The approximate positions are indicated of amino acids in F_1-ATPase that are within 4 Å of efrapeptin and help to form a largely hydrophobic interface with efrapeptin. Potential hydrogen bonds are dashed. An additional hydrogen bond (not shown) could form between the carbonyl oxygen of efrapeptin Aib-2 and the amide of αE-Val334, and there could be an electrostatic interaction between the carbonyl oxygen of efrapeptin Leu-14 and the delocalized positive charge on the heterocyclic ring of "X."

Asp356, α_E-Gln349, α_E-Phe351, and α_{TP}-Arg171 have adopted different conformers, and the main chain of the loop around α_{TP}-Thr358 has been displaced slightly.

The interactions between the antibiotic and F_1-ATPase are predominantly hydrophobic (Fig. 3). The binding of efrapeptin to *Escherichia coli* F_1-ATPase is weakened by the mutations α-Gly351Asp, α-Ser373Phe, and α-Ser375Phe (25, 26), and the mutated amino acids are equivalent to bovine residues α-Gly348, α-Ser370, and α-Ser372, respectively. Therefore, they are close to the conserved residues α-Gln349 and α-Leu369, which contribute to the hydrophobic interface between efrapeptin and subunit α_E (Fig. 3), and it is likely that the mutations perturb this region of the binding site. Two potential intermolecular hydrogen bonds can form between efrapeptin and bovine F_1-ATPase (Fig. 3). Residue α_{TP}-Arg171 also helps to form the binding site, and its situation is of particular interest, as reaction of phenylglyoxal with an unidentified arginine residue inactivates bovine F_1-ATPase, and the reaction is prevented in the F_1-ATPase–efrapeptin complex (27). Amino acid αArg-171 is the second residue in the "P-loop" that helps to bind the nucleotide (28). In subunits α_E and α_{DP}, it forms a salt bridge with Asp356 in subunits β_{DP} and β_{TP}, respectively, whereas in subunit α_{TP}, the distance of Arg171 from β_E-Asp356 is too great for a salt bridge to form, and the guanidino group is freely accessible from the central cavity. On efrapeptin binding, the solvent accessibility of α_{TP}-Arg171 decreases by 55 Å^2, six times more than any other arginine residue in the entire structural model. Therefore, α_{TP}-Arg171 may be the primary site of phenylglyoxal reaction in F_1-ATPase.

Structure of Efrapeptin. The mixture of efrapeptins coproduced by *T. inflatum* contains efrapeptins D (28%), E and F (together 44%), G (21%), H (5%), and C (2%), and a similar composition of efrapeptins was found in a crystal of the F_1-ATPase–efrapeptin complex. The crystallographic data suggest that the bound species is efrapeptin C (see Fig. 1), and there was no evidence either in the initial electron density difference map or in the map calculated from the refined model (Fig. 2*A*) for additional methyl groups in residues 4, 13, and 15, as found in various combinations in other efrapeptins (Fig. 1). Nevertheless, isovaline can be accommodated in the model at positions 4 and 15 without perturbing the structure, and conformational disorder of the additional methyl groups could explain the absence of corresponding electron density. Replacing Gly13 by alanine would require a small structural rearrangement to relieve a short contact with the carbonyl oxygen of β_E-Asp352. At the current resolution, this possibility cannot be excluded.

The atomic structure of free efrapeptin is not known. In the crystal structure of the F_1-ATPase–efrapeptin complex, the antibiotic has two rigid domains (Fig. 4) stabilized by potential intramolecular hydrogen bonds (see Fig. 3). The cyclic structure of its three pipecolic acid residues and the bulkiness of the side chain of its seven α-aminoisobutyrate residues contribute to the rigidity of the main chain, which has an unusual zig-zag secondary structure (Fig. 4). The N-terminal and C-terminal domains of efrapeptin (residues 1–6 and 9–15, respectively) are connected by a flexible region. In the free antibiotic, rotation about the single bonds in βAla-7 and Gly-8 would be virtually unrestricted, permitting the two domains to tilt and twist independently (Fig. 4). This feature is conserved in all known efrapeptins, and could help the inhibitor to reach its binding site in the core of F_1-ATPase.

Mechanism of Inhibition. According to a binding change mechanism of F_1F_o-ATP synthase (13), the conformation of an "open" catalytic β-subunit with low affinity for substrates changes during catalysis to a "closed" conformation with high affinity for the substrates ADP and phosphate. From the structure of F_1-

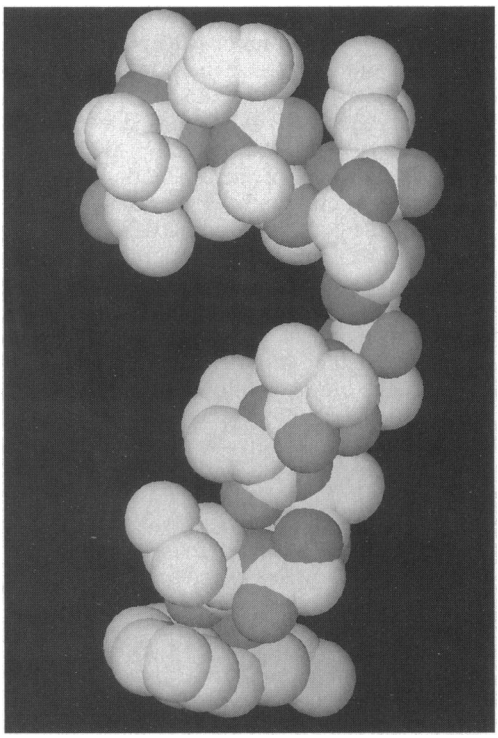

FIG. 4. Space filling representation of efrapeptin as found in the structure of the F_1-ATPase–efrapeptin complex. The two domains of the antibiotic, linked by βAla-7 and Gly-8, can twist and tilt freely.

ATPase (12) it appears likely that the "open" subunit is similar to or the same as β_E, that the "closed" conformation corresponds to those in β_{TP} and β_{DP}, and that the structural transition between them involves a hinged motion of the C terminal half (residues 364–478) of β_E inwards toward the six-fold axis of pseudo-symmetry. This movement would create a nucleotide binding domain in this subunit that is equivalent to those observed in subunits β_{TP} and β_{DP}. The structure of F_1-ATPase (12) suggests that in β_E this structural transition is prevented by the γ-subunit, which is itself held in position by the rest of the complex. Therefore, catalysis requires a concerted mechanism in which a second β-subunit adopts an "open" conformation creating an opening into which the γ-subunit can move. This rearrangement would allow subunit β_E to adopt a "closed" nucleotide binding conformation. It is postulated in the binding change mechanism (13) that all three β-subunits participate equally in catalysis, and pass through the same structural transitions during the catalytic cycle. The structure of F_1-ATPase suggests that this can be accomplished by complete rotation of the γ-subunit relative to the surrounding α- and β-subunits.

In the structure of the F_1-ATPase–efrapeptin complex, the efrapeptin is bound to a site in the core of the enzyme (Fig. 2 *B* and *C*). Part of this site is in subunit β_E between helix G (residues 321–324) and strands 3 and 7 of the β-sheet (residues 151–155 and 302–309, respectively), and the antibiotic occupies the position taken up by strand 3 in β_{TP} and β_{DP}. Other interactions of efrapeptin with subunits γ, α_E, and α_{TP} help to bind it tightly in this position (see Fig. 3). Therefore, according to the structural interpretation of the binding change mechanism described above, it would prevent the subunit from gaining the capacity to bind nucleotides, and so inhibit an essential step in both ATP hydrolysis and synthesis during the catalytic turnover of the enzyme.

The binding site of efrapeptin in F_1-ATPase does not overlap with the substrate binding sites. The competitive effect of phosphate on the rate of association of efrapeptin with F_1-ATPase (10) could arise by a conformation of the enzyme with low affinity for efrapeptins being stabilized by the binding of phosphate to an active site. Alternatively, phosphate at high concentrations could compete with efrapeptin for essential sites for binding the antibiotic. Residue α_{TP}-Arg171 is the only polar amino acid in an otherwise hydrophobic efrapeptin binding site that could provide such a site. The reactivation of ATP synthase from the efrapeptin inhibited state by high concentrations of ADP (9) could be caused by perturbation of the structure of the inhibited enzyme by ADP leading to an increased dissociation rate of the antibiotic.

The binding site of efrapeptin is the second inhibitory site to be defined in the F_1-ATPase complex. The noncompetitive inhibitor aurovertin has been shown by x-ray crystallography to bind to two equivalent sites in subunits β_{TP} and β_E in a cleft between the nucleotide and C-terminal domains (29). Therefore, these studies confirm earlier studies that showed that these two antibiotics bind at independent sites in F_1-ATPase (6). The mode of inhibition of aurovertin can also be explained in terms of the structural interpretation of the binding change mechanism. The ATPase inhibitor protein, which forms part of a regulatory mechanism of the F_1F_o-ATPase in mitochondria (30), binds to a third site in F_1-ATPase. This site, [which involves the C-terminal domain of a β-subunit (31)], the structure of the inhibitor protein, and its mode of inhibition all remain to be defined precisely by structural analysis.

We are grateful to the staff of The Synchrotron Radiation Source at Daresbury, U. K. for their help, and to Eli Lilly and Co. for providing efrapeptin. S.K.B. was supported by a long-term European Molecular Biology Organization Fellowship and M.J.v.R. was supported by a Medical Research Council Research Studentship.

1. Gupta, S., Krasnoff, S. B., Roberts, D. W., Renwick, J. A. A., Brinen, L. S. & Clardy, J. (1992) *J. Org. Chem.* **57,** 2306–2313.
2. Krasnoff, S. B. & Gupta, S. (1991) *J. Chem. Ecol.* **17,** 1953–1962.
3. Lucero, H., Lescano, W. I. M. & Vallejos, R. H. (1978) *Arch. Biochem. Biophys.* **186,** 9–14.
4. Lucero, H. A., Ravizzini, R. A. & Vallejos, R. H. (1976) *FEBS Lett.* **68,** 141–144.
5. Linnett, P. E. & Beechey, R. B. (1979) *Methods Enzymol.* **55,** 472–518.
6. Lardy, H., Reed, P. & Lin, C.-H. C. (1975) *Fed. Proc. Fed. Am. Soc. Exp. Biol.* **34,** 1707–1710.
7. Wise, J. G., Duncan, T. M., Richardson, L., Cox, D. N. & Senior, A. E. (1983) *Biochem. J.* **215,** 343–350.
8. Saishu, T., Kagawa, Y. & Shimizu, R. (1983) *Biochem. Biophys. Res. Commun.* **112,** 822–826.
9. Cross, R. L. & Kohlbrenner, W. E. (1978) *J. Biol. Chem.* **253,** 4865–4873.
10. Kohlbrenner, W. E. & Cross, R. L. (1979) *Arch. Biochem. Biophys.* **198,** 598–607.
11. Cross, R. L. (1981) *Annu. Rev. Biochem.* **50,** 681–714.
12. Abrahams, J. P., Leslie, A. G. W., Lutter, R. & Walker, J. E. (1994) *Nature (London)* **370,** 621–628.
13. Boyer, P. D. (1993) *Biochim. Biophys. Acta* **1140,** 215–250.
14. Orriss, G. L., Runswick, M. J., Collinson, I. R., Miroux, B., Fearnley, I. M., Skehel, J. M. & Walker, J. E. (1996) *Biochem. J.* **314,** 695–700.
15. Lutter, R., Abrahams, J. P., van Raaij, M. J., Todd, R. J., Lundqvist, T., Buchanan, S. K., Leslie, A. G. W. & Walker, J. E. (1993) *J. Mol. Biol.* **229,** 787–790.
16. Leslie, A. G. W. (1992) *Joint CCP4 and ESF-EACMB Newsletter on Protein Crystallography* (Daresbury Laboratory, Warrington, U.K.).
17. Collaborative Computational Project Number 4 (1994) *Acta Crystallogr. D* **50,** 760–763.
18. Tronrud, D. E., Ten Eyck, L. F. & Matthews, B. W. (1987) *Acta Crystallogr. A* **43,** 489–501.
19. Brünger, A. T. (1992) *Nature (London)* **335,** 472–475.
20. Sheriff, S. & Hendrickson, W. A. (1987) *Acta Crystallogr. A* **43,** 118–121.
21. Read, R. J. (1986) *Acta Crystallogr. A* **42,** 140–149.
22. Jones, T. A., Zou, J. Y., Cowan, S. W. & Kjeldgaard, M. (1991) *Acta Crystallogr. A* **47,** 110–119.
23. Abrahams, J. P. (1996) *Macromolecular Refinement: Proceedings of the 1996 CCP4 Study Weekend* (Daresbury Laboratory, Warrington, U.K.), in press.
24. Laskowski, R. A., MacArthur, M. W., Moss, D. S. & Thornton, J. M. (1993) *J. Appl. Crystallogr.* **26,** 283–291.
25. Wise, J. G., Latchney, L. R., Ferguson, A. M. & Senior, A. E. (1984) *Biochemistry* **23,** 1426–1432.
26. Maggio, M. B., Pagan, J., Parsonage, D., Hatch, L. & Senior, A. E. (1987) *J. Biol. Chem.* **262,** 8981–8984.
27. Kohlbrenner, W. E. & Cross, R. L. (1978) *J. Biol. Chem.* **253,** 7609–7611.
28. Walker, J. E., Saraste, M., Runswick, M. J. & Gay, N. J. (1982) *EMBO J.* **1,** 945–951.
29. van Raaij, M. J., Abrahams, J. P., Leslie, A. G. W. & Walker, J. E. (1996) *Proc. Natl. Acad. Sci. USA*, **93,** 6913–6917.
30. Walker, J. E. (1994) *Curr. Opinion Struct. Biol.* **4,** 912–918.
31. Jackson, P. J. & Harris, D. A. (1988) *FEBS Lett.* **229,** 224–228.